Chapter 3

Titanium (IV) Oxide Nanotubes in Design of Active SERS Substrates for High Sensitivity Analytical Applications: Effect of Geometrical Factors in Nanotubes and in Ag-n Deposits

Marcin Pisarek, Jan Krajczewski, Marcin Hołdyński, Tomasz Płociński, Mirosław Krawczyk, Andrzej Kudelski and Maria Janik-Czachor

Additional information is available at the end of the chapter

http://dx.doi.org/10.5772/intechopen.72739

Abstract

In this chapter, we summarize the results of recent investigations into TiO_2 nanotubular oxide layers on Ti metal loaded with Ag nanoparticles, which act as efficient surface plasmon resonators. These Ag-n/TiO_2 NT/Ti composite layers appear to be useful as platforms for precise surface analytical investigations of minute amounts of numerous types of organic molecules: pyridine (Py), mercaptobenzoic acid (MBA), 5-(4-dimethylaminobenzylidene) rhodamine (DBRh) and rhodamine (R6G); such investigations are known as surface enhanced Raman Spectroscopy (SERS). Geometrical factors related to the nanotubes and the silver deposit affect the SERS activity of the resulting composite layers. The results presented here show that, for a carefully controlled amount of Ag-n deposit located mainly on the tops of titania nanotubes, it is possible to obtain high-quality, reproducible SERS spectra for probe molecules at an enhancement factor of 10^5–10^6. This achievement makes it possible to detect organic molecules at concentrations as low as, e.g., 10^{-9} M for R6G molecules. SEM investigations suggest that the size of the nanotubes, and both the lateral and perpendicular distribution of Ag-n (on the tube tops and walls), are responsible for the SERS activity. These features of the Ag-n/TiO_2 NT/Ti composite layer provide a variety of cavities and slits which function as suitable resonators for the adsorbed molecules.

Keywords: TiO_2 nanotubes (TiO_2 NT), Ag nanoparticles (Ag-n), PVD methods of Ag-n deposition, SERS measurements, enhancement factor (E_F)

1. Introduction

Searching for new and effective substrates for surface enhanced Raman Spectroscopy (SERS) applications is a subject of research at many scientific centers. This is because SERS spectroscopy is used to quickly characterize many functional materials important in advanced technologies, analytical chemistry and biology [1]. An important practical problem when carrying out analytical SERS measurements is to obtain suitable substrates containing a sufficient number of electromagnetic nanoresonators. The SERS effect is strongly dependent on an enhancement of the Raman scattering intensity by molecules adsorbed on a nanostructured metallic surface. The SERS enhancement factor is related to the size and shape of the nanostructures, which causes electromagnetic enhancement [2, 3]. Usually, the average value of SERS enhancement is around 10^5–10^6, but localized enhancement may reach values of 10^{10} at certain, highly efficient sub-wavelength regions of the surface [4]. It is therefore desirable for the resulting substrates to render a very large SERS spectra enhancement factor, where the enhancement factor thus obtained does not depend on where the measurement is made (the same enhancement factor should be present at different locations on the sample surface [5]).

A promising substrate for SERS measurements that meets these two most important practical requirements is regular TiO_2 nanotubes loaded with metal nanoparticles, which support surface plasmon resonance. One way of modifying the nanotubular layer and attaining high SERS activity is to enhance the surface with a small quantity of Ag or other plasmonic metal (e.g. Au or Cu) nanoparticles (plasmonic nanoparticles) [1, 6]. Such plasmonic metals themselves are known for their high SERS activity, which results only after a proper roughening of their surfaces [7]. The dielectric constant for these metals consists of a negative real part and a small positive imaginary part. When a nanoparticle made of these metals interacts with electromagnetic radiation, collective oscillations of the surface plasmons are induced [8]. These oscillations result in an enhanced electromagnetic field in close proximity to the surface of the nanoparticles. The surface of these metals, when properly roughened, provides suitable slits and cavities which serve as surface plasmon resonators that strongly enhance the intensity of the electromagnetic field. For Raman bands with a small Raman shift, the increase in the efficiency of Raman scattering is roughly proportional to the fourth power of the field enhancement [2, 9]. A detailed description of the SERS effect can be found in literature [2, 9–12].

It is well known that the enhancement factor (E_F) of SERS spectra depends on the metal morphology/topography. Only a suitable surface roughness of the SERS substrates can produce a stronger Raman signal. The optimum value of the size and shape of the noble metal particles may lead to a maximum E_F (which also depends on the nature of the metal, the excitation laser wavelength, and special experimental conditions) [13]. A highly active substrate provides superior conditions for measuring the SERS spectra of an adsorbate. Therefore, to gain some insight into the substrate–adsorbate interactions at the molecular level, and to detect different kinds of organic adsorbates, detailed knowledge of how to fabricate a highly sensitive and reproducible SERS substrate is of considerable importance [1, 5].

The high regularity of the TiO_2 nanotubular structures obtained ensures that the enhancement factors are high reproducible [14–16]. The specific morphology of the resulting structures (the large side wall surfaces of the nanotubes grown perpendicular to the substrate) makes it possible to prepare metallic nanograin systems with a large number of gaps between the

http://dx.doi.org/10.5772/intechopen.72739

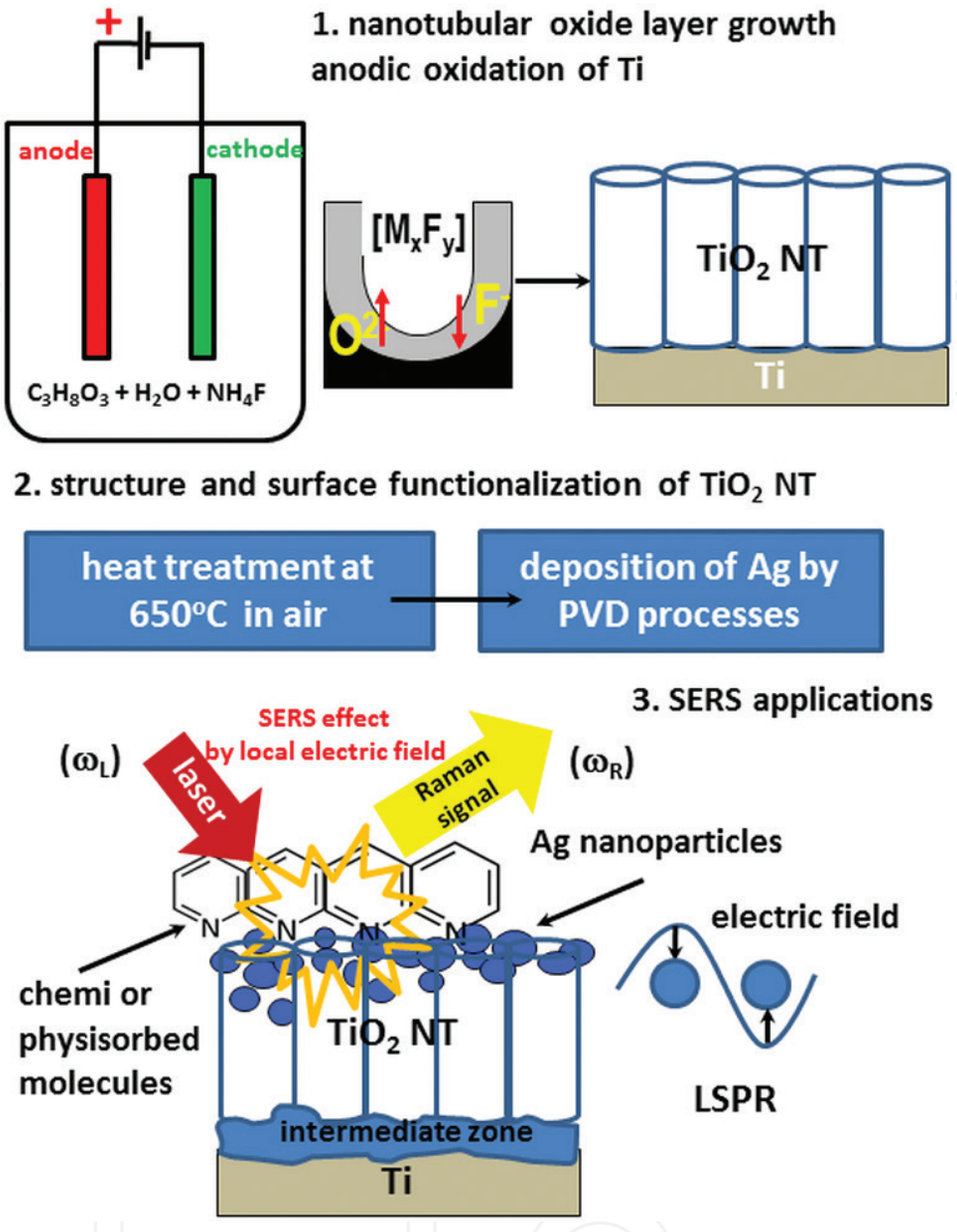

Figure 1. Schematic presentation of fabrication of TiO_2 nanotube layer and functionalization process for SERS application.

nanotubes (i.e. the metal nanoparticle systems are close to each other on the side walls of TiO_2 nanotubes that are perpendicular to the macroscopic Ti surface). As shown experimentally, the narrow gaps between the metal nanoparticles supporting surface plasmon resonance produce the largest SERS signal enhancement factors [17–19] (see **Figure 1**).

In this chapter we discuss in more detail the effect of a TiO_2 nanoporous structure with Ag nanoparticles deposited by different PVD methods (which provide precise control over the amount of silver sputtered onto the nanotubular substrate) on the SERS activity of the substrates prepared. We focus on the geometrical effects on SERS activity: nanotube diameter, size and distribution of Ag-n, and morphology of the Ag-n agglomerates. TiO_2 nanotubes are particularly suitable for such investigations because the strictly controlled electrochemical procedures make it possible to produce well-formed, nanotubular substrates that are "homogeneous," statistically having the same nanotube diameter and nanotube wall thickness (see **Figure 2**).

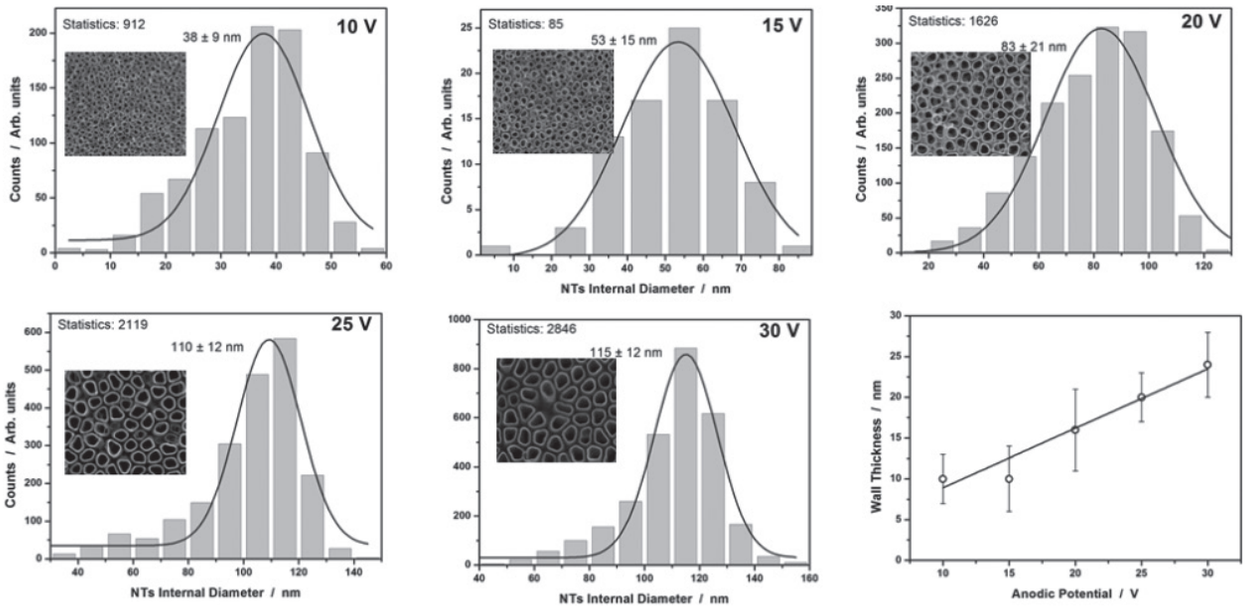

Figure 2. Effect of anodic voltage V_{max} on average diameter and wall thickness of nanotubes. The inserts show top views of TiO_2 nanotubes fabricated at different voltages [21].

As shown in **Figure 2**, the specific morphology of TiO_2 nanotubes can be relatively easily modified by controlling the conditions of anodic polarization (type of electrolyte, voltage and anodization time), because there is a direct linear relationship between anodization voltage and the average diameter of the nanotubes formed. In general, the diameter and wall thickness of the nanotubes increase with anodic voltage [20, 21]. The possibility of preparing nanotubes of different size, shape and wall thickness provides control over the geometrical surface area and specific surface area, which are important parameters when developing new substrates for SERS applications.

2. Fabrication, surface and structure characterization of SERS substrates based on TiO_2 nanotubes

Innovative SERS active platforms based on TiO_2 NT with noble metal deposits (Ag) were used for investigating various organic probe molecules such as pyridine (Py), mercaptobenzoic acid (MBA), organic dye 5-(4-dimethylaminobenzylidene) rhodamine (DBRh) and rhodamine 6G (R6G). For this purpose, simple electrochemical methods were applied: anodic oxidation of Ti foil (0.25 mm-thick, 99.5% purity, Alfa Aesar) in an optimized electrolyte: a glycerol/water mixture (volume ratio 50:50) with 0.27 M NH_4F under different constant voltages from 10 up to 30 V. They led to the formation of nanoporous titanium oxide structures, and subsequently, to the preparation of specific metal nanostructures on surfaces thereof during PVD processes (magnetron sputtering, evaporation at high and low vacuum). Before the Ag deposition, all of the samples were annealed in air at 650°C for 3 h in order to transform the structure of the TiO_2 NT from amorphous to crystalline [19, 22].

Ag nanoparticles (from 0.01 up to 0.03 mg/cm^2) were deposited using the sputter deposition technique: the evaporation method in a low vacuum ($p = 3 \times 10^{-3}$ Pa) with a JEE-4X JEOL

device, and the DC magnetron sputtering technique using a Leica EM MED020 apparatus in a configuration perpendicular to the surface of the samples. More details are given elsewhere [18, 23]. We strictly controlled in situ the average amount of metal deposited per cm^2 using a quartz microbalance. One has to consider, however, that the true local amount of the metal deposits may vary substantially from site to site. The highly developed specific surface area of the nanotube arrays and its brush-like morphology may strongly affect Ag local distribution, resulting in considerable non-uniformity. For this type of process, silver targets of 99.9% purity (Kurt J. Lesker Company) were used. To better control the silver sputtering deposition process on the surface of the nanotubes, we applied the thermal evaporation method (0.01 and 0.05 mg/cm^2) using an EF 40C1 effusion cell inside an UHV preparation chamber (PREVAC, Poland). The cell was maintained at a temperature of 900°C during the process of resistive evaporation. Silver (2 mm-diameter wire, 99.999%, Alfa Aesar) was evaporated onto the room temperature-surface of the TiO_2 NT at a pressure of $1–2 \cdot 10^{-6}$ Pa at a constant evaporation rate of 0.13 nm/min. The evaporation rate from the silver effusion cell was calibrated and monitored using a TM-400 quartz crystal thickness monitor (Maxtek Inc.). The process of fabricating the SERS substrates is presented schematically in **Figure 1**.

The SERS platforms thus fabricated were characterized using various analytical methods. Electron Microscopy was applied for the morphological and structural characterization of the nanotubes after each preparation stage. The SEM observations (FEI NovaNanoSEM 450, Hitachi S70, Hitachi S-5500) were carried out at an accelerating voltage of 5 or 10 kV and an SE detector to reveal topographic contrast at the tops of the tubes. The thin sample for STEM observations was prepared by using the lift-out technique with a Hitachi NB-5000Focused Ion Beam system. The internal structure of the nanotubes was examined with a dedicated STEM Hitachi HD2700 in BF and atomic mass contrast. Observations at 200 kV revealed a columnar structure of the nanotubes and the transition zone. The surface chemical composition and the chemical state of the surface species (Ti, O, Ag) of the fabricated SERS platforms were examined using XPS spectroscopy. The XPS spectra were measured with a Microlab 350 Thermo Electron spectrometer at 300 W non-monochromatic Al K_α radiation and 1486.6 eV energy. AES spectroscopy was applied to determine the local chemical composition of the SERS substrates obtained. All of the spectra were recorded at an energy of 10 kV. The appropriate standards for AES and XPS reference spectra were also used. Finally, the Raman spectra of 2-mercaptoethanesulfonate (5×10^{-3} M), pyridine (5×10^{-2} M, in a mixture of pyridine and 0.1 M KCl), DBRh (10^{-4} M, in a mixture of water and ethanol (1:2)), and rhodamine from a 10^{-7} and 10^{-9} M aqueous solution were collected with a Horiba Jobin–Yvon Labram HR800 using a He-Ne laser (632.8 nm) as the excitation source. For each sample, 20 measurements were performed locally at various points chosen randomly.

3. Results and discussion

For our studies, we used an optimized electrolyte based on a mixture of glycerol and water (volume ratio 50:50) with 0.27 M NH_4F. The growth of nanotubes under a constant voltage is perpendicular to the metal substrate, as shown in **Figure 3**. STEM images reveal nanotubes that are hollow in shape, separated from each other, and that feature a characteristic

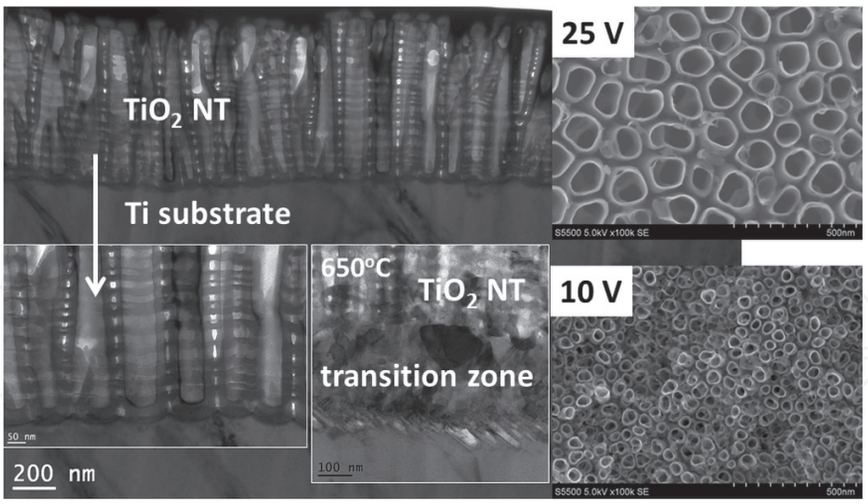

Figure 3. STEM images of a cross-section of a TiO_2 nanotubular layer before and after heat treatment at 650°C (20 V); insert shows a top view of the nanotubes obtained at 25 and 10 V.

"columnar structure." A typical surface morphology of the nanotubes is shown in the inset to **Figure 3** (10 and 25 V). Usually, the as-grown porous anodic layers exhibit poor adhesion to the Ti substrate, and so, to improve their adhesion and mechanical stability, the samples were annealed in air at 650°C for 3 h. The heat treatment in this temperature range does not cause any visible changes in the diameter or shape of the TiO_2 nanotubes, but in the annealing process an interfacial region is formed between the Ti substrate and the TiO_2 nanotubes that stabilizes the entire TiO_2 NT/Ti substrate system. Moreover, the heat treatment results in a change in the nanotube structure, from amorphous (directly after anodization) to crystalline: anatase [19, 21, 24]. All these factors are crucial for the suitability of the nanotubes as substrates when preparing SERS-active adsorbates.

After annealing, the above structures proved to be important for designing active substrates for SERS spectroscopy, where a large surface area and a stabilized structure are required [19]. The free-standing nanotubes adorned with Ag nanoparticles formed a layer of natural nanoresonators (antennas), which repeatedly enhanced Raman scattering [14, 18]. However, the geometrical factors of the Ag-n deposit and their relation to the geometry of the nanotubes are not yet well understood. Therefore, the details of the SERS mechanism should be carefully considered.

In general, there are two important mechanisms underlying SERS. The first, and the dominant, mechanism toward large SERS enhancement factors (E_F) is that of electromagnetic field enhancement, where localized surface plasmons (LSPs) in the metallic nanostructure increase the Raman signal intensity. The other contribution to SERS E_F is the chemical enhancement mechanism, where the charge transfer between the adsorbed molecule and the metal plays a critical role in enhancing and modifying the modes of molecular vibration [25]. Both enhancement mechanisms can operate simultaneously when using TiO_2 nanoporous structures in the form of freestanding nanotubes with a suitable, carefully prepared deposit of silver nanoparticles.

Figure 4 shows SEM images of TiO_2 nanotube layers (top-views) formed at 25 V and loaded with 0.01 mg/cm^2 of Ag. A careful inspection of **Figure 4a** reveals that the magnetron-deposited Ag-n is located on the tops and side walls of the nanotubes, while the silver particles become

http://dx.doi.org/10.5772/intechopen.72739

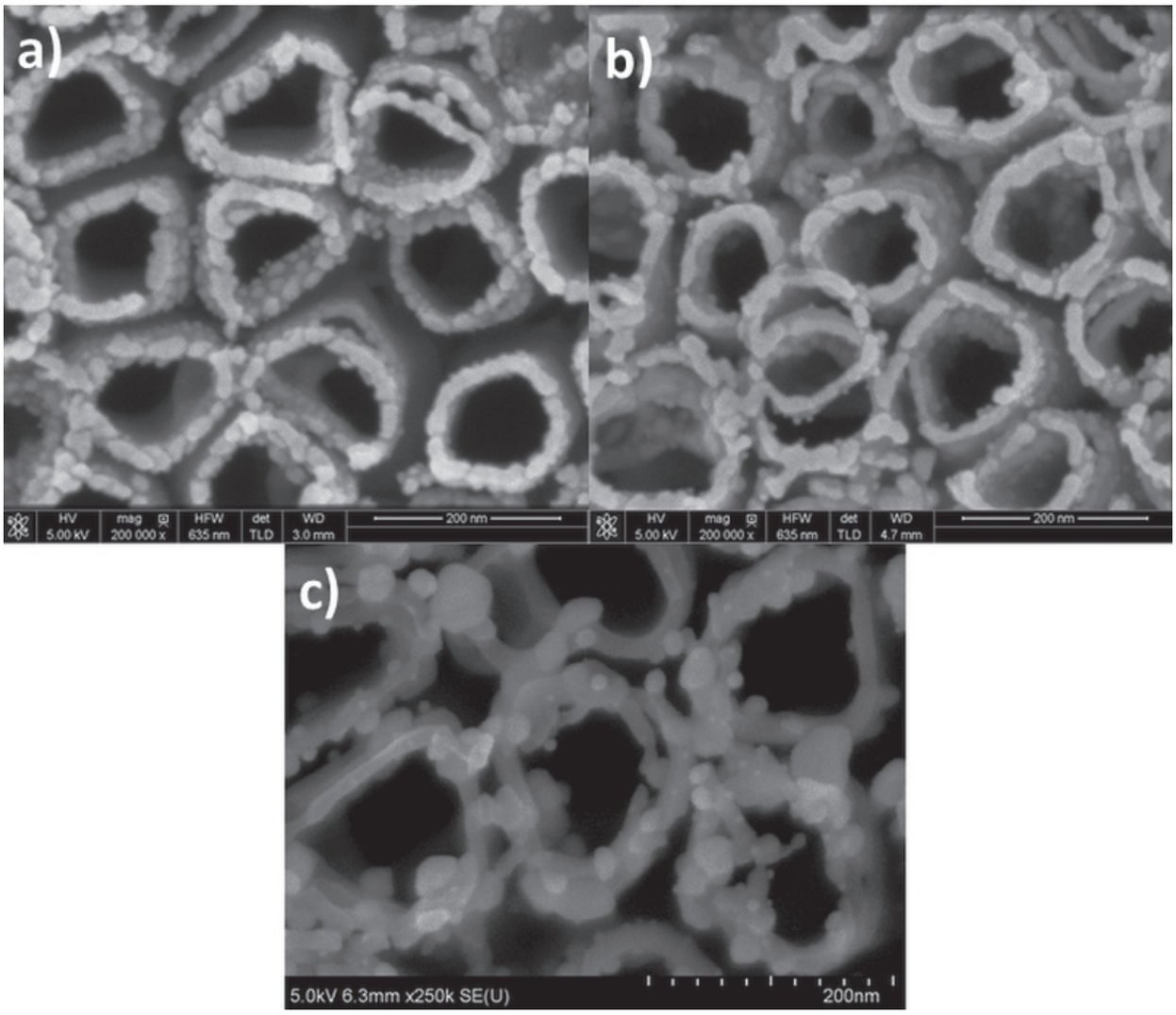

Figure 4. SEM images of TiO_2 nanotube layers (top-views) formed at 25 V and loaded with 0.01 mg Ag/cm^2 after different PVD processes: (a) magnetron sputtering, (b) evaporation at a low vacuum, and (c) evaporation at a high vacuum.

agglomerated and form rings. As a result of silver evaporation at a low vacuum, the plasmonic nanoparticles are distributed homogenously in the TiO_2 nanotube layer, tightly covering the walls of the nanotubes and forming a thin, solid coating around the tubes (**Figure 4b**). After evaporation at a high vacuum, where the process of silver deposition is very slow (0.13 nm/min), spherical Ag nanoparticles are formed (see **Figure 4c**). The diameter of these particles is below 50 nm. Densely-packed TiO_2 nanotubes coated with a plasmonic metal (Ag) could act as antenna-nanoresonators having a strictly defined geometry and surface development. This would ensure the formation of highly active places—"hot spots," i.e., gaps and cavities serving as surface plasmon resonators that significantly increase the intensity of the electromagnetic field.

Figure 5 shows typical AES spectra for samples with an Ag deposit (0.01 mg/cm^2) after vacuum evaporation at low and high vapor pressures. Signals from the Ag MNN, Ti LMM and O KLL Auger transitions are clearly visible. These results suggest that O is bound to Ti, and there are areas where the oxidized Ti substrate is not fully covered by the Ag deposit, which is consistent with the SEM microscopic observations.

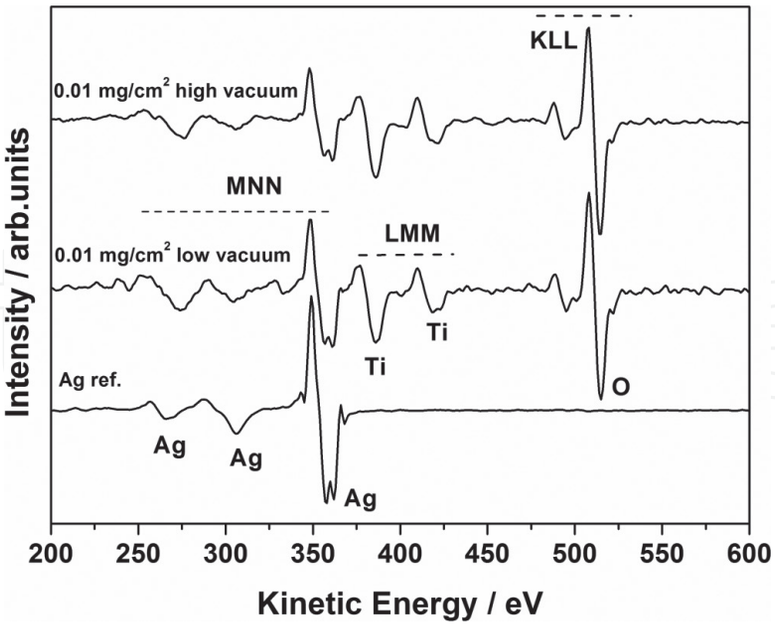

Figure 5. Typical Auger survey spectra taken at the surface of Ag/TiO_2 NT layers obtained at V_{max} = 25 V and covered with the same amount of Ag deposit (0.01 mg/cm^2). The Ag MNN signal for a pure Ag reference sample is also shown.

In order to gain further insight into the chemical state of the samples before and after the silver deposition processes, XPS measurements were performed for those samples having a small amount of Ag (0.01 mg/cm^2) (see **Table 1**). The deconvolution of the main XPS signals for $Ti2p_{3/2}$ and O1s suggests that titanium is bound to oxygen and forms titanium oxide IV. High-resolution XPS spectra confined to the Ag range gave the binding energies of $Ag3d_{5/2}$ peaks located at 367.9 (high vacuum), 368.3 (magnetron sputtering) and 368.4 eV (low vacuum), respectively, which is consistent with the literature [26–30] and also with our reference data. This implies that the Ag agglomerates and single nanoparticles located on the tops and in the deeper parts of the TiO_2 nanotubes are metallic silver. A small shift in the $Ag3d_{5/2}$ and $Ti2p_{3/2}$ peaks (see **Table 1**) for the samples after functionalization by PVD methods (±0.1–0.4 eV) may suggest that the XPS signals of Ag are modified by an interaction with the TiO_2 nanoporous substrate in relation to the position of the Ag standard peak. This interaction may induce a shift in the Fermi level in the deposited silver, in particular, if single nanoparticles are supported on the oxide carrier – the SMSI effect. Such effects have been reported by Goodman et al. and Lopez et al. [31, 32] for gold nanoparticles on TiO_2 supports, and were also observed in our recent work, where a ZrO_2 nanoporous layer was covered with Ag nanoparticles [33].

Figure 6 shows the SERS spectra of pyridine (Py) adsorbed at TiO_2 NT/Ti platforms fabricated at 25 V and covered with the same average amount of Ag-n (0.01 mg/cm^2) by the three different procedures: magnetron sputtering, and vacuum evaporation at low and high vapor pressures. The spectra presented were averaged from 20 measurements on each sample tested. The SERS spectra of pyridine are dominated by two bands: at ~1010 and at ~1034 cm^{-1} originating from the aromatic ring vibrations of this molecule. Moreover, on the spectra recorded, there are also others bands clearly visible at 1150 and 1220 cm^{-1}, which are also characteristic of Py adsorbed on a standard silver surface [34, 35]. The SERS measurements revealed that the distribution of Ag nanoparticles on the nanotubular substrate affects SERS intensity (compare

samples	Peak	BE / eV	Chemical Bond
25V TiO_2 NT / 650°C [in this work]	$Ti2p_{3/2}$	459.0	Ti-O (TiO_2)
	O1s	530.2	Ti-O (TiO_2)
25V TiO_2 NT / 650°C + thin Ag film (magnetron sputtering) [in this work]	$Ti2p_{3/2}$	459.3	Ti-O (TiO_2)
	O1s	530.6	Ti-O (TiO_2)
	$Ag3d_{5/2}$	368.3	Ag metal
25V TiO_2 NT / 650°C + thin Ag film (evaporation method at low vacuum) [in this work]	$Ti2p_{3/2}$	459.1 and 459.3	Ti-O (TiO_2)
	O1s	530.5 and 530.6	Ti-O (TiO_2)
	$Ag3d_{5/2}$	368.1 and 368.4	Ag metal
25V TiO_2 NT / 650°C + Ag single nanoparticles (evaporation method at high vacuum) [in this work]	$Ti2p_{3/2}$	459.1	Ti-O (TiO_2)
	O1s	530.4	Ti-O (TiO_2)
	$Ag3d_{5/2}$	367.9	Ag metal
Reference materials			
Titanium dioxide [20]	$Ti2p_{3/2}$	458.8	Ti-O (TiO_2)
Silver foil ref. material [in this work]	$Ag3d_{5/2}$	368.2	Ag metal
Silver metal [20]	$Ag3d_{5/2}$	368.3	Ag metal

Table 1. XPS results for titania nanotube layers before and after silver nanoparticles deposition by PVD methods at low and high vacuums.

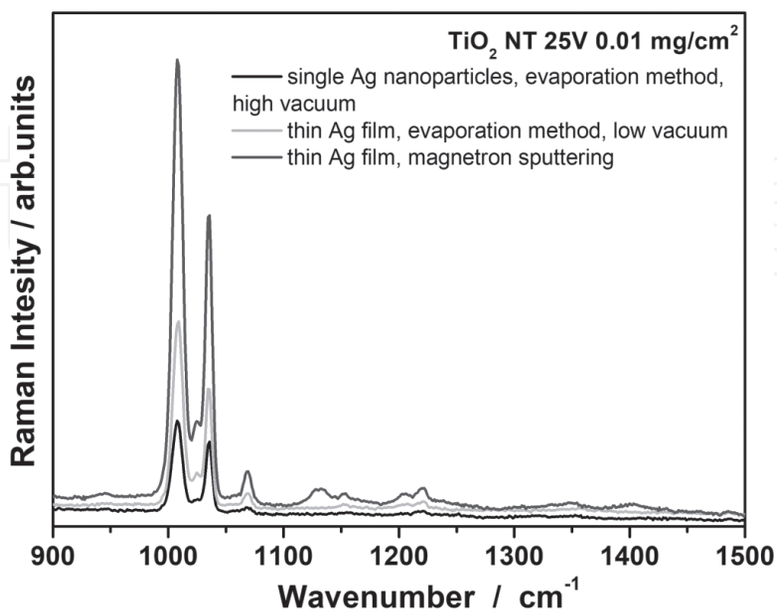

Figure 6. Average SERS spectra of Py adsorbed on Ag-n/TiO_2NT (25 V)/Ti substrates fabricated by: Ag magnetron sputtering, Ag evaporation method at a low vacuum, Ag thermal evaporation method at a high vacuum.

Figure 4). A roughly two-fold increase in SERS intensity occurs when the titania nanotubes are adorned with Ag-n after the magnetron sputtering process. Three kinds of Ag particles can be distinguished: those accumulated on the tops of the nanotubes, forming "rings," and single particles (see. **Figure 4**) separated from each other and/or those Ag particles produced in the high vacuum process, which are located on the tops ("mouth") of the nanotubes. The latter do not yield such a strong SERS effect. Apparently, the key factor in the SERS activity of Ag-n *is the size and mode of the specific surface area of the silver particles* formed during a specific vacuum process. While the SERS intensity reached was not very high, well-reproducible and good-quality SERS spectra were obtained.

The next step was to repeat the same measurements with a nanotubular substrate prepared at an anodization of 10 V to produce nanotubes having a smaller diameter, thereby increasing the specific surface area of the SERS-active silver. **Figure 7** shows typical SEM images of a platform for SERS measurements, based on TiO_2 nanotubes (10 V): a surface of nanotubes of titania on a Ti substrate after deposition of Ag nanoparticles by the evaporation method in a low vacuum of 0.01 (a), 0.02 (b), and 0.03 (d) mg Ag/cm^2. For the smallest amount of Ag (0.01 mg·cm^{-2}), the silver nanoparticles tend to gather on the tops of the nanotubes and on their side walls (c). Characteristic specific structures of Ag-n are formed around the nanotubes, consisting of agglomerates of Ag nanoparticles. Increasing the amount of silver (0.02 and 0.03 mg·cm^{-2}) leads further to a visible development of the Ag surface area, up to the formation of silver nanoparticle agglomerates having characteristic slits of from several to a few dozen nanometers.

Figure 8 shows the spectrum of pyridine adsorbed on Ag-n/TiO_2 NT (10 V) platforms from an aqueous solution of 0.05 M pyridine +0.1 M KCl. The spectra are dominated by two strong

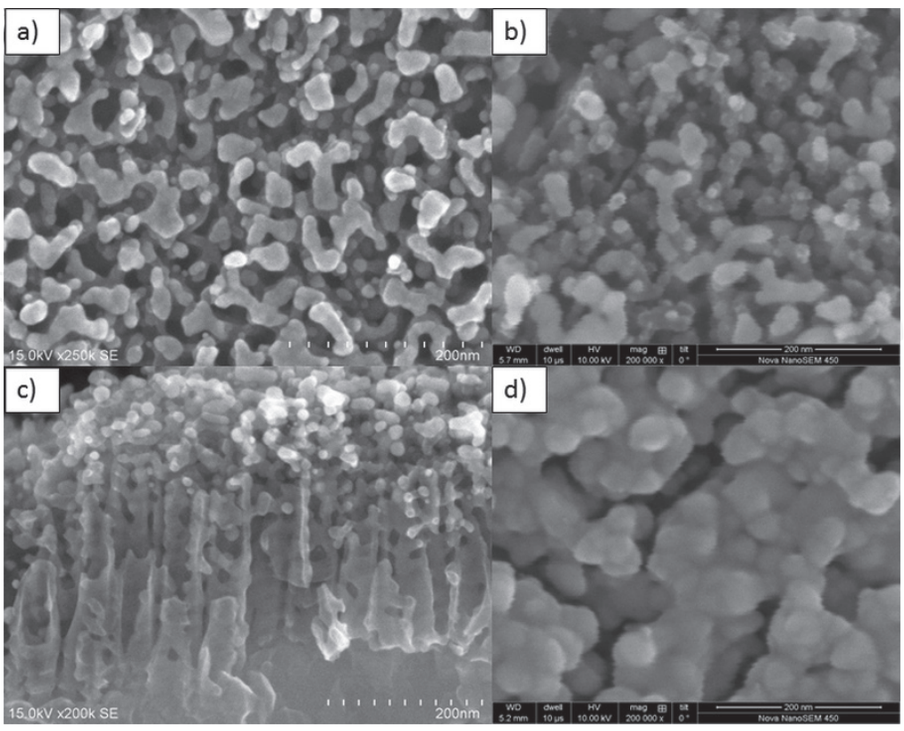

Figure 7. Top view of titania dioxide nanotubes (10 V) annealed for 2 h in air at a temperature of 650°C after silver deposition: 0.01 (a), 0.02 (b), 0.03 mg/cm^2 (d). A cross-sectional view of a nanoporous layer after deposition of Ag – 0.01 mg/cm^2 is also given, left side (c).

bands at 1004 and 1034 cm^{-1}. The band at 1004 cm^{-1} is due to the ring breathing mode (ν_1, Wilson notation), whereas that at 1034 cm^{-1} is due to symmetric triangular ring deformation (ν_{12}) [34, 35]. The SERS spectral intensity increases distinctly with the amount of Ag metal deposit, which correlates with a change in surface topography (compare **Figure 7**). This effect is most likely related to an increase in the number of narrow gaps between the silver particles themselves (locations particularly active in SERS spectroscopy) with an increasing amount of Ag deposit.

Our previous experiments show that the SERS enhancement factor for free-standing TiO_2 nanotubes adorned with silver nanoparticles is strictly related to the size of the nanotubes. The SERS enhancement factor (E_F) for the pyridine (Py) probe molecule was successfully estimated using the following formula (1):

$$E_F = I_{SERS}/I_{ref} \times hc_{ref}/N_{surf} \quad (1)$$

where I_{SERS} and I_{ref} are the Raman intensities obtained from the SERS and normal Raman (NR) investigations, respectively, c_{ref} stands for the concentration of pure Py in the NR measurements, and h is the depth-of-focus of the laser beam. The average number of adsorbed molecules of Py per geometrical surface area unit participating in the SERS measurements (N_{surf}) was calculated assuming that the adsorbed molecules are spheres closely packed on a plane to form a hexagonal lattice. AFM measurements were performed to determine the geometrical surface area, see **Figure 9a**. More details can be found in the publication [15].

For the same amount of Ag deposit (0.02 mg/cm^2, magnetron sputtering) on nanotubes fabricated at 10 V up to 25 V (see **Figure 2**), there was an increase in the SERS enhancement factor of from 10^5 to 10^6 (see **Figure 9b**).

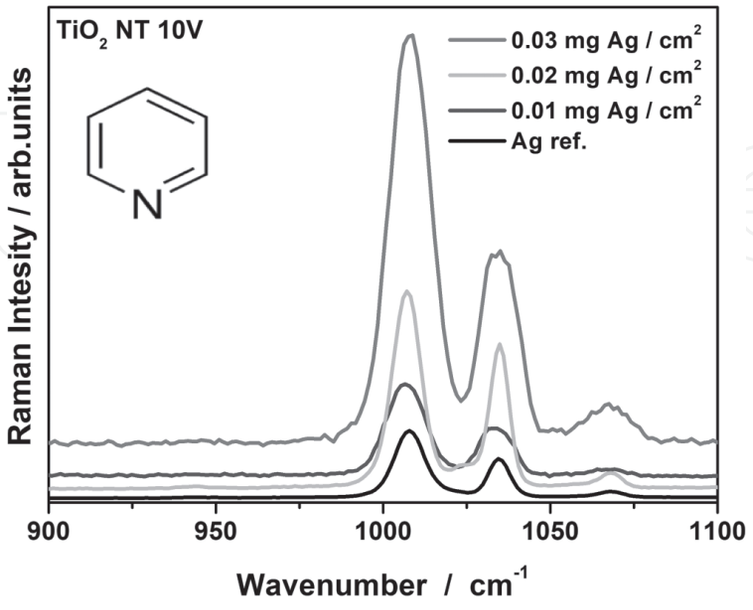

Figure 8. SERS spectra of pyridine adsorbed at the surface of nanotubes (10 V) annealed in air at 650°C for 2 h and coated with silver deposit: 0.01, 0.02, 0.03 mg/cm^2. A reference spectrum for pure Ag (electrochemically roughened silver surface) is also given.

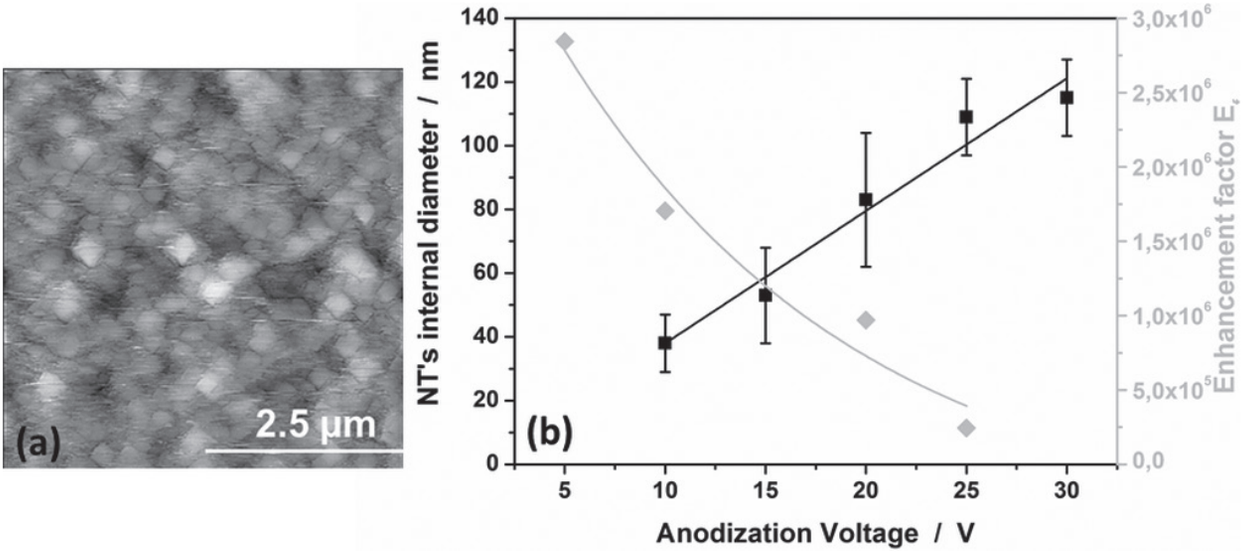

Figure 9. (a) Typical AFM image of silver nanoparticles (0.020 mg/cm^2) deposited by the magnetron sputtering technique on TiO_2 oxide layers (20 V)—top view; (b) SERS enhancement factor E_F as a function of the final formation voltage V_{max} of the titania nanoporous layers. E_F estimated for Py band at ~1010 cm^{-1}, Ag deposited by magnetron sputtering technique—0.02 mg/cm^2.

The hundredfold increase in SERS enhancement shown in **Figure 9b** is apparently due to a combination of two factors: a change in the specific surface area of the nanotubes with formation voltage [15], and a change in the distribution and size of the Ag nanoparticles with nanotube size [23]. These geometrical factors affect the properties of the silver "nanoresonators" produced on the tops and side walls of the TiO_2 nanotubes. The present results confirm the importance of the size of the geometrical surface area of the TiO_2 nanotubes for the plasmonic properties of the Ag-n deposit itself and, consequently, for the properties of the Ag/TiO_2NT composite materials.

Figure 10 shows SERS spectra of two other probe molecules: p-mercaptobenzoic acid (a) and DBRh dye (b) recorded on the platforms, which were characterized by an enhancement factor larger than 10^6. In both cases, the spectra are of good quality and high intensity. They show that the background is not very high, and quite "flat" for both molecules. Our SERS experiments confirmed the good reproducibility of such substrates obtained by adorning TiO_2 nanotubes with Ag metal clusters and particles, which effectively support plasmon resonance [18].

Figures 11 and **12** show R6G spectra taken with our Ag-n/TiO_2 NT platform covered with a solution containing 10^{-7} or 10^{-9} mol/l R6G. A rhodamine molecule is often used when the relationship between the local electromagnetic field enhancement and a large SERS signal is explored, which makes it possible to measure Raman spectra from a single molecule located on an Ag particle or individual Ag nanoparticles [36–39]. The characteristic peaks at ~970, 1150, 1220, 1300, 1340, 1410, 1500 and 1600 cm^{-1} correspond to the Raman lines for R6G [3, 36]. In particular, the bands which are usually assigned to aromatic C-C stretching vibrations of R6G molecule are clearly visible. It can be seen that the SERS spectrum of R6G adsorbed on our Ag substrate exhibits enough intensity for this molecule to be detected even at a small concentration in an aqueous solution (below 10^{-7} mol/l). As a result of this reduced concentration of R6G, some bands are suppressed (compare **Figures 11** and **12**). This sensitivity of our

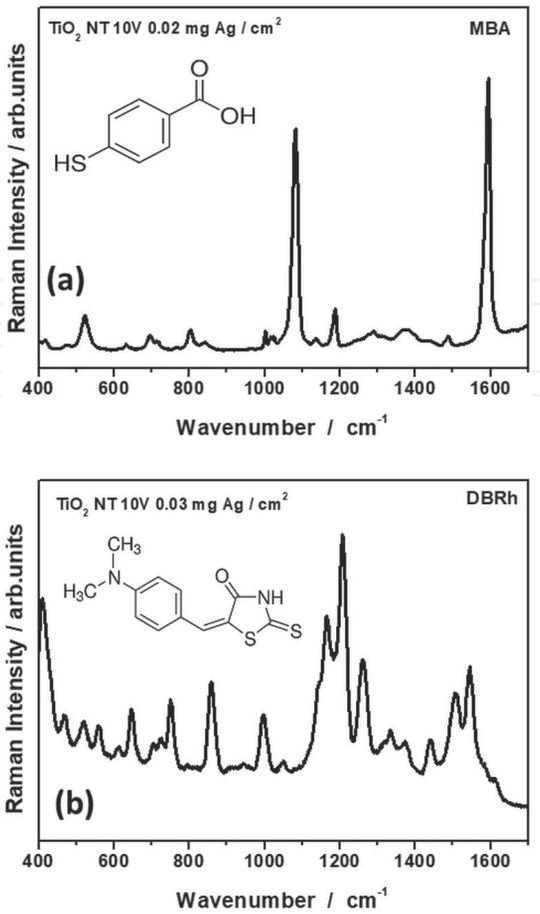

Figure 10. SERS spectra of p-mercaptobenzoic acid (a) and DBRh dye (b) recorded at the surface of 10 V nanotubes.

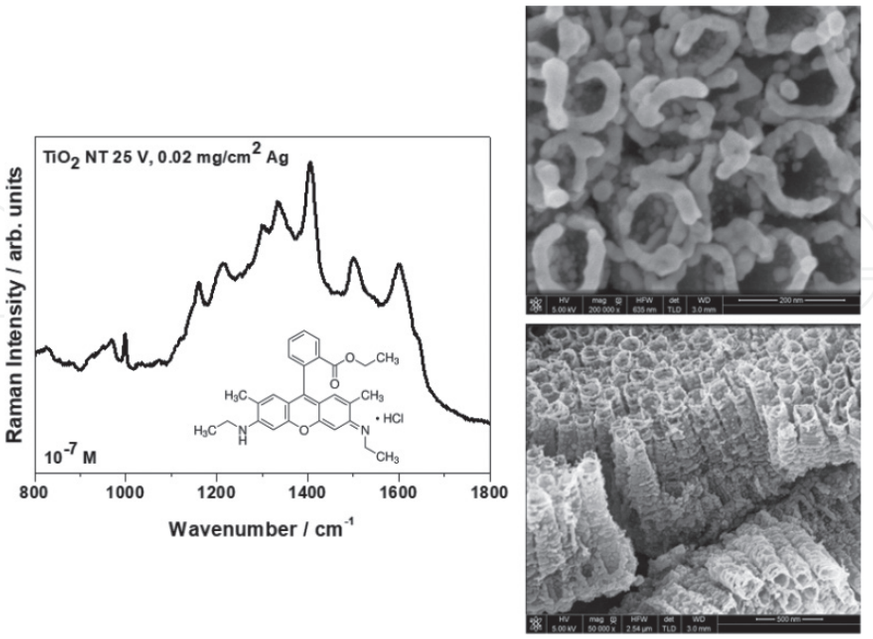

Figure 11. Left: SERS spectrum for R6G molecules adsorbed from an 10^{-7} M aqueous solution on a surface of TiO_2 NT nanotubes (25 V) with a silver deposit of 0.02 mg/cm² (magnetron sputtering). Right: SEM images showing the morphology and cross-sectional view of the SERS active platform.

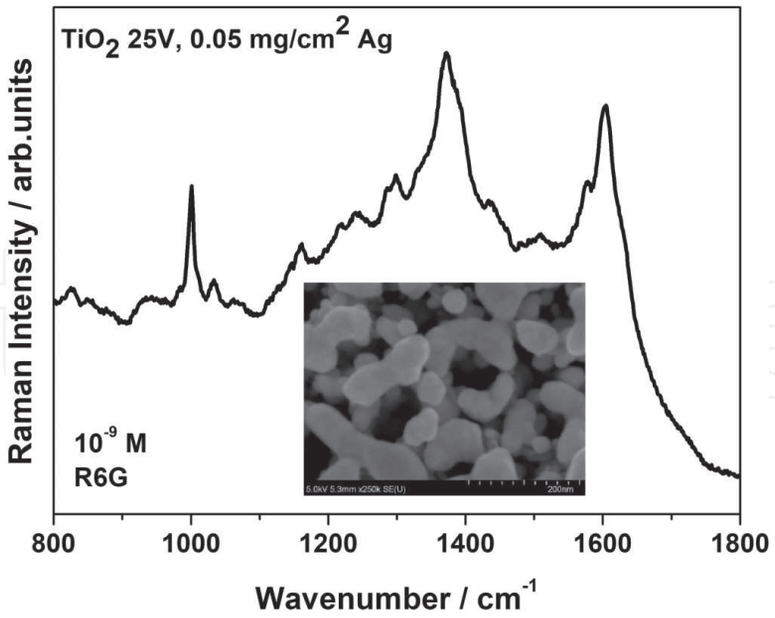

Figure 12. SERS spectrum of R6G molecules adsorbed from a 10^{-9} M aqueous solution on a surface of TiO_2 NT nanotubes (25 V) with a silver deposit of 0.05 mg/cm^2 (thermal evaporation method at a high vacuum).

fabricated SERS substrates is apparently related to the homogeneous Ag distribution on the surface of the regular nanoporous TiO_2 structures; this should make it possible to produce specific morphologies that are extremely useful in Raman investigations.

4. Conclusions and outlook

PVD methods (the sputtering technique) provide a strictly controlled, stable distribution of Ag-n on nanotubular titania, thus offering suitable platforms for SERS investigations and for measurements of high-quality SERS spectra. Such spectra were obtained for pyridine, p-mercaptobenzoic acid, rhodamine and rhodamine 6G dye adsorbed on Ag-n-functionalized nanoporous layers of titania. For the SERS measurements (with R6G), excellent spectra were obtained, even for a concentration of R6G in a solution as low as 10^{-9} mol/l. The E_F value was found to be the largest ($E_F = 2.8 \times 10^6$) for the smallest nanotube diameter (d = 38 ± 9 nm). Stable, reproducible and highly active platforms for SERS investigations were obtained using relatively simple procedures and techniques.

The SERS enhancement induced by these new materials is associated primarily with two geometric factors: the specific surface area of the nanotubes, and an appropriate size and distribution of the Ag nanoparticles. These geometric factors (clearly visible using high-resolution microscopy) affect the properties of the metallic "nanoresonators" deposited on the TiO_2 nanotubes. Consequently, the probe molecules sense even slight changes on the surface, and these manifest themselves in the SERS intensity. However, the spectral differences observed result not only from the specific morphology, where the PVD techniques lead to the formation of cavities and slits that operate as adsorbed molecule resonators, but also from a specific interaction between the Ag nanoparticles and the TiO_2 nanotubes themselves. The further

development of this type of SERS platform may involve using Ti of varying degrees of purity, and alloys of Ti, where the impurities and alloying elements will have an impact on the formation of nanoporous oxides layers by means of doping process (a change in the electron structure of the titanium oxide). As a consequence, this could lead to a significantly stronger enhancement of the intensity of the SERS spectra due to the occurrence of modified interactions between the doped titanium oxide and the metal nanoparticles, effectively supporting surface plasmons resonance (Ag, Au, Cu). All those factors should be taken into account when planning future analytical applications of new modified SERS substrates.

Acknowledgements

We are most grateful to Prof. Robert Nowakowski from the Institute of Physical Chemistry PAS (Poland) for his cooperation (AFM measurements) and many helpful discussions. This work was financially supported by the Institute of Physical Chemistry PAS.

Author details

Marcin Pisarek[1]*, Jan Krajczewski[2], Marcin Hołdyński[1], Tomasz Płociński[3], Mirosław Krawczyk[1], Andrzej Kudelski[2] and Maria Janik-Czachor[1]

*Address all correspondence to: mpisarek@ichf.edu.pl

1 Institute of Physical Chemistry, Polish Academy of Sciences, Warsaw, Poland

2 Faculty of Chemistry, University of Warsaw, Warsaw, Poland

3 Faculty of Material Science and Engineering, Warsaw University of Technology, Warsaw, Poland

References

[1] Sharma B, Frontiera RR, Henry AI, Ringe E, Van Duyne RP. SERS materials, applications, and the future. Materials Today. 2012;**15**:16-25. DOI: 10.1016/S1369-7021(12)70017-2

[2] Schlucker S. Surface-enhanced Raman spectroscopy: Concepts and chemical applications. Angewandte Chemie, International Edition. 2014;**53**:4756-4795. DOI: 10.1002/anie.201205748

[3] Tian F, Bonnier F, Casey A, Shanahan AE, Byrne HJ. Surface enhanced Raman scattering with gold nanoparticles: Effects of particle shape. Analytical Methods. 2014;**6**:9116-9123. DOI: 10.1039/c4ay02112f

[4] Fan M, Andrade GFS, Brolo AG. A review on the fabrication of substrates for surface enhanced Raman spectroscopy and their applications in analytical chemistry. Analytica Chimica Acta. 2011;**693**:7-25. DOI: 10.1016/j.aca.2011.03.002

[5] Cialla D, Marz A, Bohme R, Theil F, Weber K, Schmitt M, Popp J. Surface-enhanced Raman spectroscopy (SERS): Progress and trends. Analytical and Bioanalytical Chemistry. 2012;**403**:27-54. DOI: 10.1007/s00216-011-5631-x

[6] Krajczewski J, Kołątaj K, Kudelski A. Plasmonic nanoparticles in chemical analysis. RSC Advances. 2017;**7**:17559-17576. DOI: 10.1039/c7ra01034f

[7] Jeanmaire DL, Van Duyne RP. Surface raman spectroelectrochemistry: Part I. Heterocyclic, aromatic, and aliphatic amines adsorbed on the anodized silver electrode. Journal of Electroanalytical Chemistry. 1977;**84**:1-20. DOI: 10.1016/S0022-0728(77)80224-6

[8] Yamamoto YS, Ozaki Y, Itoh T. Recent progress and frontiers in the electromagnetic mechanism of surface-enhanced Raman scattering. Journal of Photochemistry & Photobiology, C: Photochemistry Reviews. 2014;**21**:81-104. DOI: 10.1016/j.jphotochemrev.2014.10.001

[9] Ding SY, You EM, Tian ZQ, Moskovits M. Electromagnetic theories of surface-enhanced Raman spectroscopy. Chemical Society Reviews. 2017;**46**:4042-4076. DOI: 10.1039/c7cs 00238f

[10] Stiles PL, Dieringer JA, Shah NC, Van Duyne RP. Surface-enhanced Raman spectroscopy. Annual Review of Analytical Chemistry. 2008;**1**:601-626. DOI: 10.1146/annurev. anchem.1.031207.112814

[11] Chen X-J, Cabello G, Wu D-Y, Tian Z-Q. Surface-enhanced Raman spectroscopy toward application in plasmonic photocatalysis on metal nanostructures. Journal of Photochemistry and Photobiology C: Photochemistry Reviews. 2014;**21**:54-80. DOI: 10.1016/j.jphotochemrev.2014.10.003

[12] Kudelski A. Raman spectroscopy of surfaces. Surface Science. 2009;**603**:1328-1334. DOI: 10.1016/j.susc.2008.11.039

[13] Du Y, Shi L, He T, Sun X, Mo Y. SERS enhancement dependence on the diameter and aspect ratio of silver-nanowire array fabricated by anodic aluminium oxide template. Applied Surface Science. 2008;**255**:1901-1905. DOI: 10.1016/j.apsusc.2008.06.140

[14] Roguska A, Kudelski A, Pisarek M, Opara M, Janik-Czachor M. Surface-enhanced Raman scattering (SERS) activity of Ag, Au and Cu nanoclusters on TiO_2-nanotubes/Ti substrate. Applied Surface Science. 2011;**257**:8182-8189. DOI: 10.1016/j.apsusc.2010.12.048

[15] Pisarek M, Hołdyński M, Roguska A, Kudelski A, Janik-Czachor M. TiO_2 and Al_2O_3 nanoporous oxide layers decorated with silver nanoparticles – Active substrates for SERS measurements. Journal of Solid State Electrochemistry. 2014;**18**:3099-3109. DOI: 10.1007/s10008-013-2375-x

[16] Pisarek M, Roguska A, Kudelski A, Hołdyński M, Janik-Czachor M: Ch.17: Self-organized TiO_2, Al_2O_3 and ZrO_2 nanotubular layers: Properties and applications. In: Aliofkhazraei M editor. Comprehensive Guide for Nanocoatings Technology, Vol.3. New York Nova Science Publishers, Inc. 2015. p. 435-462, ISBN:978-1-63482-647-1

[17] Lamberti A, Virga A, Chiado A, Chiodoni A, Bejtka K, Rivolo P, Giorgis F. Ultrasensitive Ag-coated TiO_2 nanotube arrays for flexible SERS-based optofluidic devices. Journal of Materials Chemistry C. 2015;**3**:6868-6875. DOI: 10.1039/c5tc01154j

[18] Kudelski A, Pisarek M, Roguska A, Hołdyński M, Janik-Czachor M. Surface-enhanced Raman scattering investigations on silver nanoparticles deposited on alumina and titania nanotubes: Influence of the substrate material on surface-enhanced Raman scattering activity of Ag nanoparticles. Journal of Raman Specroscopy. 2012;**43**:1360-1366. DOI: 10.1002/jrs.4075

[19] Pisarek M, Roguska A, Kudelski A, Andrzejczuk M, Janik-Czachor M, Kurzydlowski KJ. The role of Ag particles deposited on TiO_2 or Al_2O_3 self-organized nanoporous layers in their behavior as SERS-active and biomedical substrates. Materials Chemistry and Physics. 2013;**139**:55-65. DOI: 10.1016/j.matchemphys.2012.11.076

[20] Lee K, Mazare A, Schmuki P. One-dimensional titanium dioxide nanomaterials: Nanotubes. Chemical Reviews. 2014;**114**:9385-9454. DOI: 10.1021/cr500061m

[21] Roguska A, Pisarek M, Belcarz A, Marcon L, Hołdyński M, Andrzejczuk M, Janik-Czachor M. Improvement of the bio-functional properties of TiO_2 nanotubes. Applied Surface Science. 2016;**388**:775-785. DOI: 10.1016/j.apsusc.2016.03.128

[22] Roguska A, Pisarek M, Andrzejczuk M, Dolata M, Lewandowska M, Janik-Czachor M. Characterization of a calcium phosphate – TiO_2 nanotube composite layer for biomedical applications. Materials Science and Engineering: C. 2011;**31**:906-914. DOI: 10.1016/j.msec.2011.02.009

[23] Pisarek M, Nowakowski R, Kudelski A, Hołdyński M, Roguska A, Janik-Czachor M, Kurowska-Tabor E, Sulka GD. Surface modification of nanoporous alumina layers by deposition of Ag nanoparticles. Effect of alumina pore diameter on the morphology of silver deposit and its influence on SERS activity. Applied Surface Science. 2015;**357**:1736-1742. DOI: 10.1016/j.apsusc.2015.10.011

[24] Regonini D, Bowen CR, Jaroenworaluck A, Stevens R. Effect of heat treatment on the properties and structure of TiO_2 nanotubes: Phase composition and chemical composition. Materials Science and Engineering R. 2013;**74**:377-406. DOI: 10.1016/j.mser.2013.10.001

[25] Wang AX, Kong X. Review of recent progress of Plasmonic materials and nano-structures for surface-enhanced Raman scattering. Materials. 2015;**8**:3024-3052. DOI: 10.3390/ma8063024

[26] Edited by Chastain J, King Jr. RC: Handbook of X-Ray Photoelectron Spectroscopy, a Reference Book of Standard Spectra for Identification and Interpretation of XPS Data. Physical Electronics, Inc. Eden Praire; 1995. ISBN 0-9648124-1-X

[27] Kumar R, Rashid J, Barakat MA. Zero valent Ag deposited TiO_2 for the efficient photocatalysis of methylene blue under UV-C light irradiation. Colloids and Interface Science Communications. 2015;**5**:1-4. DOI: 10.1016/j.colcom.2015.05.001

[28] Gross PA, Pronkin SN, Cottineau T, Keller N, Keller V, Savinova ER. Effect of deposition of Ag nanoparticles on photoelectrocatalytic activity of vertically aligned TiO_2 nanotubes. Catalysis Today. 2012;**189**:93-100. DOI: 10.1016/j.cattod.2012.03.054

[29] Zhang J, Li Y, Zhang Y, Chen M, Wang L, Zhang C, He H. Effect of support on the activity of Ag-based catalysts for formaldehyde oxidation. Scientific Reports. 2015;**5**:12950. DOI: 10.1038/srep12950

[30] Albiter E, Valenzuela MA, Alfaro S, Valverde-Aguilar G, Martinez-Pallares FM. Photocatalytic deposition of Ag nanoparticles on TiO_2: Metal precursor effect on the structural and photoactivity properties. Journal of Saudi Chemical Society. 2015;**19**:563-573. DOI: 10.1016/j.jscs.2015.05.009

[31] Goodman DW. "Catalytically active Au on Titania": Yet another example of a strong metal support interaction (SMSI)? Catalysis Letters. 2005;**99**(1-2):1-4. DOI: 1011-372X/05/0100-0001/0

[32] Lopez N, Nørskov JK. Theoretical study of the Au/TiO_2(110) interface. Surface Science. 2002;**515**:175-186 S00 39-6028 (02) 01873- 3

[33] Pisarek M, Krajczewski J, Wierzbicka E, Hołdyński M, Sulka GD, Nowakowski R, Kudelski A, Janik-Czachor M. Influence of the silver deposition method on the activity of platforms for chemometric surface-enhanced Raman scattering measurements: Silver films on ZrO_2 nanopore arrays. Spectrochimica Acta – Part A: Molecular and Biomolecular Spectroscopy. 2017;**182**:124-129. DOI: 10.1016/j.saa.2017.04.005

[34] Zuo C, Jagodzinski PW. Surface-enhanced Raman scattering of pyridine using different metals: Differences and explanation based on selective formation of α-Pyridyl on metal surfaces. The Journal of Physical Chemistry. B. 2005;**109**:1788-1793. DOI: 10.1021/jp0406363

[35] DY W, Li JF, Ren B, Tian ZQ. Electrochemical surface-enhanced Raman spectroscopy of nanostructures. Chemical Society Reviews. 2008;**37**:1025-1041. DOI: 10.1039/b707872m

[36] Michaels AM, Nirmal M, Brus LE. Surface enhanced Raman spectroscopy of individual Rhodamine 6G molecules on large Ag Nanocrystals. Journal of the American Chemical Society. 1999;**121**:9932-9939. DOI: 10.1021/ja992128q

[37] Liu YC, ChCh Y, Sheu SF. Low concentration rhodamine 6G observed by surface-enhanced Raman scattering on optimally electrochemically roughened silver substrates. Journal of Materials Chemistry. 2006;**16**:3546-3551. DOI: 10.1039/b609417a

[38] Dieringer JA, Wustholz KL, Masiello DJ, Camden JP, Kleinman SL, Schatz GC, Van Duyne RP. Surface-enhanced Raman excitation spectroscopy of a single Rhodamine 6G molecule. Journal of the American Chemical Society. 2009;**131**:849-854. DOI: 10.1021/ja8080154

[39] Pristinski D, Tan S, Erol M, Du HSS. In situ SERS study of Rhodamine 6G adsorbed on individually immobilized Ag nanoparticles. Journal of Raman Specroscopy. 2006;**37**:762-770. DOI: 10.1002/jrs.1496